Two-dimensional Non-linear Microwave Imaging with Total Variation Regularization

K. Yaswanth and Uday K. Khankhoje
Electrical Engineering, Indian Institute of Technology Madras, Chennai 600036, India

Abstract— Using an electric field integral equation formulation, we perform a comparative study between linear and nonlinear microwave imaging with adaptive total variation regularization. It is well known that linearized methods fail for higher values of dielectric contrasts. So, it is important to investigate nonlinear methods which are valid for higher contrasts. However, these methods have the challenge of dealing with computationally expensive computations of the cost-function gradients; in this paper, we propose a fast gradient computation using the conjugate-gradient fast Fourier transform. Further, we impose a total variation based regularization where the regularization parameter is adaptively estimated using a Bayesian approach, and minimize the cost function using a majorization-minimization algorithm. Finally, we compare the performance and computational costs of using the nonlinear optimization method.

1. INTRODUCTION

Inverse microwave imaging is a technique where we get information about the scatterer by measuring scattered Electric fields using multiple transceivers. Inverse microwave imaging techniques have huge potential in biomedical imaging, subsurface object detection, concealed weapon detection, nondestructive testing and evaluation. Frequently used methods of microwave imaging are Born Iterative method (BIM) [8], Distorted Born Iterative Method (DBIM) [4] and Contrast Source Inversion (CSI) [5], which use linear gradients in their formulations. We have nonlinear gradient methods [2] which are exact for all contrasts. In all the above specified methods regularization is to be done, as the problem is ill conditioned and ill-posed. Regularizations like L1-norm [6], L2-norm [3], Total-Variation (TV) [7], Joint L1-L2 [8], etc. are adopted to make the problem well-posed. In this paper, we perform a comparative study between linear and nonlinear gradient methods using Iterative method (IM) with TV regularization in the 2D transverse magnetic case. The paper is organized as follows. Section 2 describes the problem formulation. Section 3 explains the inversion techniques used to solve the inverse problem, where we discuss the nonlinear and linear methods, and the total variation technique of regularization. In Section 4, results are discussed and we conclude in Section 5.

2. PROBLEM FORMULATION

Let us consider a two-dimensional problem as shown Fig. 1. Where the scatterer is the object of interest (OI), Domain of interest (D) is the region where we know that the scatterer exists, measurement domain (S) is where the transceivers are placed. Electric field integral equation (EFIE) is used to solve this problem as shown in Eq. (1).

$$E_j^{Scat}(\vec{r}) = E_j(\vec{r}) - E_j^{inc}(\vec{r}) = k_b^2 \iint\limits_D G(\vec{r} - \vec{r'})[\epsilon_r(\vec{r'}) - 1]E_j(\vec{r'})dv(\vec{r'}) \tag{1}$$

where $E_j(\vec{r})$, $E_j^{inc}(\vec{r})$ and $E_j^{scat}(\vec{r})$ are the total, incident and scattererd electric fields, respectively, at point '$\vec{r}$' when jth transmitter is transmitting. $G(\vec{r}, \vec{r'})$ is the 2D free space Green's function. $\epsilon_r(\vec{r})$ is the relative permittivity, k_b is wavenumber of the homogenous medium in which the scatterer and transceivers are present.

We can discretize the Domain of interest into 'n' equal grids and 'm' transceivers are uniformly placed in the measurement domain. On discretizing Eq. (1) with $\vec{r}, \vec{r'} \in D$, we get Object Eq. (3) and with $\vec{r} \in S$, $\vec{r'} \in D$, we get the data Eq. (2) [9].

$$s_j = G_1 U_j x = G_1 X u_j \tag{2}$$

$$e_j = (I - G_0 X) u_j \tag{3}$$

where s_j, u_j, $x = \epsilon_r - 1$ and e_j are column vectors of sizes $m \times 1$, $n \times 1$, $n \times 1$ and $n \times 1$, respectively. They denote scattered fields at receivers, internal electric fields inside scatterer (unknown), contrast

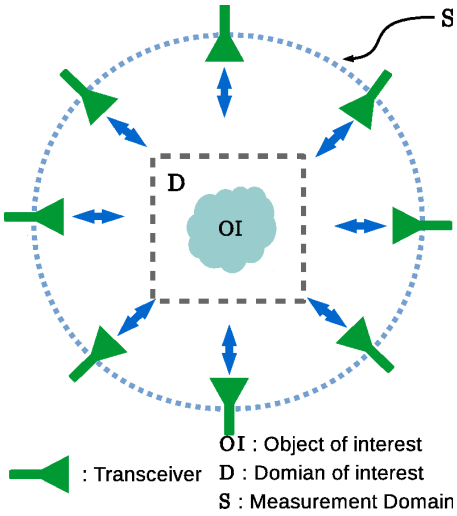

Figure 1: Problem setup.

inside scatterer (unknown) and incident electric fields inside the scatterer (known), respectively, when the jth transmitter is transmitting. G_1 and G_0 are matrices with integrals of Green's function of size $m \times n$ and $n \times n$, respectively. X and U_j are diagonal forms of x and u_j column vectors, i.e., $X = \text{diag}(x)$.

3. INVERSION TECHNIQUE

As we can see from Eq. (2), the scattered electric field is a function of both contrast (x) and total electric field (u) of the scatterer. We can solve for contrast by using Iterative method (IM) using the algorithm shown in Fig. 2. The forward problem is solved using conjugate gradient fast Fourier transform (CG-FFT) [10].

1: **procedure** INVERSION ALGORITHM ▷ Algorithm to find the object contrast
2: **Initialize** G_0, G_1, e_j, s_j
3: **Initialize** $u_j \leftarrow e_j$ ▷ Born approximation
4: **Estimate** x ▷ Initial guess
5: **while** Convergence not achieved **do**
6: **Find** u_j ▷ Solve forward problem in Eq. (3)
7: **Estimate** x ▷ Contrast update minimizing Eq. (4)
8: **end while**
9: **end procedure**

Figure 2: Pseudocode for inversion algorithm

The cost function to be minimized to update the contrast (x) is shown in Eq. (4),

$$F(x, x^*) = \sum_{j=1}^{m} ||G_1 X u_j - \widetilde{s}_j|\,|^2 + \gamma R(x, x^*) \tag{4}$$

where $R(x, x^*)$ is the regularization term, $\widetilde{s}_j$ is column vector of scattered field measured at receivers (known), γ is the weight and '$*$' implies a conjugate variable.

In gradient methods like the steepest descent and conjugate gradient, the gradient of the cost function is calculated by taking internal fields to be independent of x as in Eq. (5) or dependent as in Eq. (6), which we call as linear and nonlinear gradients, respectively. Linear gradient is an approximation which is used widely in literature [5, 6, 8], whereas Non-linear gradient [2] is exact but less used, as a matrix inversion operation has to be performed. In this paper, the matrix

inversion operation is implemented using CG-FFT to reduce the computational time.

$$\nabla^{L}_{x^*} F(x, x^*) = \sum_{j=1}^{m} U_j^{\dagger} G_1^{\dagger} (G_1 U_j x - \widetilde{s}_j) + \gamma \nabla_{x^*} R(x, x^*) \tag{5}$$

$$\nabla^{NL}_{x^*} F(x, x^*) = \sum_{j=1}^{m} \left[U_j^{\dagger} + U_j^{\dagger} G_0^{\dagger} \left(I - X^{\dagger} G_0^{\dagger} \right)^{-1} X^{\dagger} \right] G_1^{\dagger} (G_1 U_j x - \widetilde{s}_j) + \gamma \nabla_{x^*} R(x, x^*) \tag{6}$$

where '†' is conjugate transpose.

3.1. Total Variation Regularization

Total variation regularization term $R(x, x^*)$ is used, as seen in Eq. (7). The final cost function is minimized using maximization and minimization algorithm [7] and the weight γ is estimated using a Bayesian approach [7].

$$R(x, x^*) = TV(x) = \sum_{i=1}^{n} \sqrt{|\Delta_i^h x|^2 + |\Delta_i^v x|^2} \tag{7}$$

where $\gamma = \frac{2(\alpha+\theta N)\sigma^2}{TV(x_0)+\beta}$, σ^2 is the variance of the noise, and α and β are constants, such that $\alpha \ll \theta N$ and $TV(x) \gg \beta$.

4. RESULTS

A comparative study of linear and nonlinear gradients was done using the object shown in Fig. 3 with domain size of $1\lambda \times 1\lambda$, discretization of $\lambda/40$ for synthetic data and $\lambda/20$ for inverse problem. Measurements were taken using 10 transceivers on a circle of radius equal to 4λ. We can see a left sided semicircle of radius $5\lambda/16$ and center $(-\lambda/8, 0)$ has contrast of $x1$ and a square of side length $\lambda/5$ and center $(\lambda/5, 0)$ with contrast $x2$. To understand the behaviour, we have assumed the shape of the scatterer to be known and only their contrasts, $x1$ and $x2$, to be unknown. In Fig. 4, contours represent the cost function for different combinations of $x1$ and $x2$. Many saddle points, local minimas and local maximas are observed. Figs. 4(a), (c) correspond to linear gradients and Figs. 4(b), (d) correspond to nonlinear gradients. The negative of both linear and nonlinear gradients are arrows which have to point in the direction to minimize the cost function, respectively with their lengths proportional to their magnitutes. In Figs. 4(a), (b), we have the true contrast of scatterer $x1$ and $x2$ to be 0.5 and 0.5, respectively. In linear case, negative of the linear gradient deviates from what is expected at high contrast values. In nonlinear case, negative of nonlinear gradient always points towards steepest descent direction and initial guess decides to which local minima solution converges. Similar behaviour has been observed in low contrast scatterers. So, in case of low contrast objects, both linear and nonlinear gradient methods gives similar results, if started with a very low initial guess. In Figs. 4(c), (d), we have true contrasts of scatterer, $x1$ and $x2$, to be 3 and 7, respectively, which are high in magnitute. From Fig. 4(c), It is observed

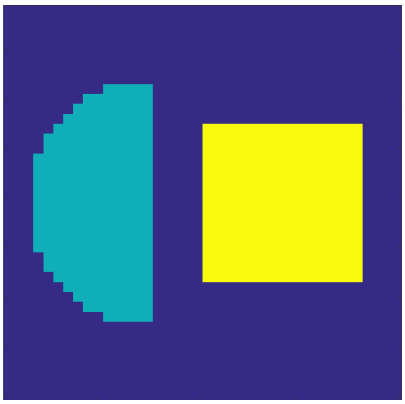

Figure 3: Domain size = $1\lambda \times 1\lambda$, discretization is $\lambda/40$ for synthetic problem and $\lambda/20$ for inverse problem, measurement radius = 4λ.

that, starting from low contrast values than the true value will never reach to global minima in linear case. In the region around the true solution, all the negatives of linear gradients are not pointing towards the true solution. So, linear methods will never converge to the true solution. In Fig. 4(d) we observe that starting near the true solution will guarantee convergence to the global minima. So, we need to start will multiple starting points to reach global optimum. We need to answer the question, how many starting points should we start with in nonlinear case? For the case of Figs. 4(b), (d), solution converged to global minimum with probability 0.21 and 0.48, respectively, where we started with random starting points within the box constraint of $x1 \in [0, 10]$ and $x2 \in [0, 10]$ in the presence of 20 dB SNR.

In Fig. 5(a) is the actual modified Austria profile [12] used in a domain of $2\lambda \times 2\lambda$, with a ring centered at $(0, -\lambda/5)$ of inner and outer radius $3\lambda/10$ and $\lambda/2$, respectively and two other circles of radius $\lambda/5$ centered at $(\lambda/2, 3\lambda/5)$ and $(-\lambda/2, 3\lambda/5)$ respectively with contrast 1. 27

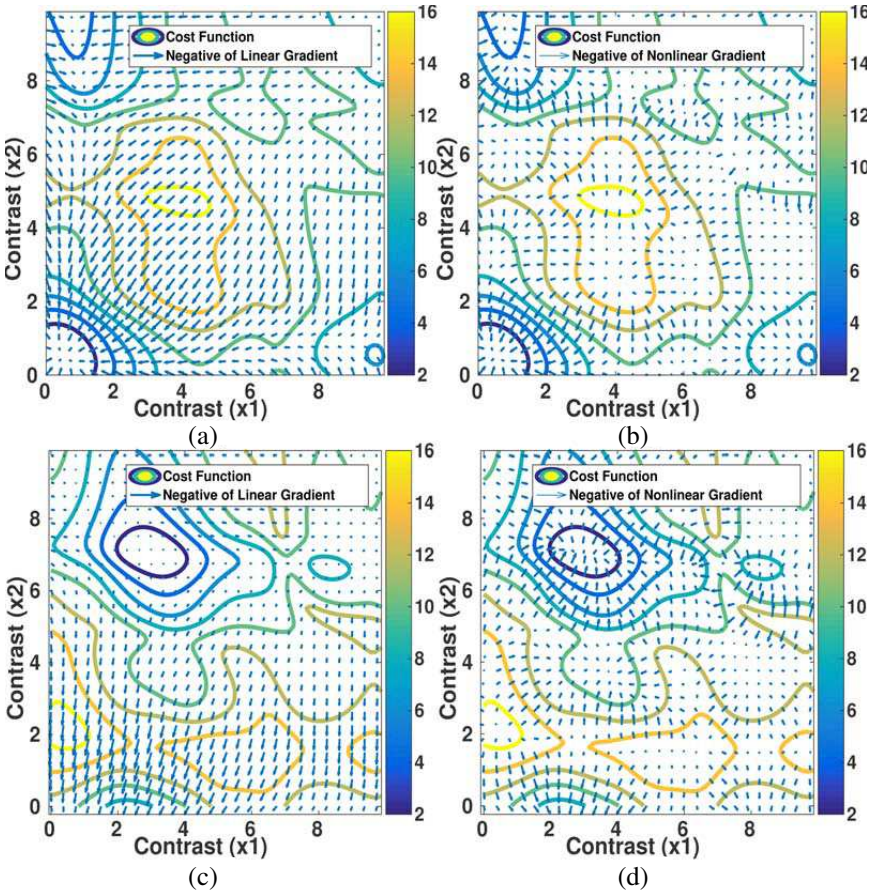

Figure 4: Domain size = $1\lambda \times 1\lambda$, discretization is $\lambda/40$ for synthetic data and $\lambda/40$ for inverse problem, measurement radius = 4λ.

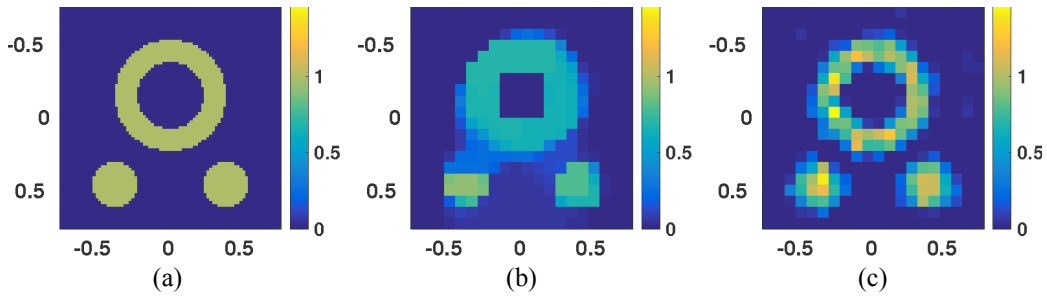

Figure 5: (a) Actual object with contrast 1, in a domain of size $2\lambda \times 2\lambda$, illuminated by 27 trans-receivers, (b) and (c) demonstrate reconstructions using linear and nonlinear methods with costs (L2 norm) of 0.1649 and 0.065; and shape errors of 10% and 6%, respectively.

transceivers are placed at a circle of radius 4λ to take the scattering measurements. Gaussian noise of 20 dB is added to the measurements; (b) and (c) are the reconstructed contrast profiles using linear and nonlinear methods using total variation regularization and maximization and minimization algorithm. Linear and nonlinear methods took 48 and 262 seconds of computational time, respectively, with resconstruction errors of 10% and 6%, respectively. Computational cost per iteration are of orders n^2 and $n^2 \log n$ for linear and nonlinear methods, respectively.

5. CONCLUSION

A fast CG-FFT based nonlinear gradient method has been presented for solving 2D inverse scattering problems and was compared with linear gradient methods. The results have shown that linear gradient methods are limited to low contrast object reconstructions and nonlinear methods have to be used if we need to solve for higher contrasts. They are implemented using total variation regularization and maximization-minimization algorithm. The results show that the linear methods are less accurate compared to nonlinear methods. The computational complexity of linear methods and fast CG-FFT based nonlinear methods are of order n^2 and $n^2 \log n$ per iteration, respectively.

REFERENCES

1. Rubek, T., et al., "Nonlinear microwave imaging for breast-cancer screening using Gauss-Newton's method and the CGLS inversion algorithm," *IEEE Transactions on Antennas and Propagation*, Vol. 55, No. 8, 2320–2331, 2007.
2. Franchois, A. and C. Pichot, "Microwave imaging-complex permittivity reconstruction with a Levenberg-Marquardt method," *IEEE Transactions on Antennas and Propagation*, Vol. 45, No. 2, 203–215, 1997.
3. Colton, D., H. Haddar, and M. Piana, "The linear sampling method in inverse electromagnetic scattering theory," *Inverse Problems*, Vol. 19, No. 6, S105, 2003.
4. Chew, W. C. and Y.-M. Wang, "Reconstruction of two-dimensional permittivity distribution using the distorted born iterative method," *IEEE Transactions on Medical Imaging*, Vol. 9, No. 2, 218–225, 1990.
5. Van Den Berg, P. M. and R. E. Kleinman, "A contrast source inversion method," *Inverse problems*, Vol. 13, No. 6, 1607, 1997.
6. Ambrosanio, M. and V. Pascazio, "A compressive-sensing-based approach for the detection and characterization of buried objects," *IEEE Journal of Selected Topics in Applied Earth Observations and Remote Sensing*, Vol. 8, No. 7, 3386–3395, 2015.
7. Oliveira, J. P., J. M. Bioucas-Dias, and M. A. T. Figueiredo, "Adaptive total variation image deblurring: A majorization-minimization approach," *Signal Processing*, Vol. 89, No. 9, 1683–1693, 2009.
8. Shah, P., U. K. Khankhoje, and M. Moghaddam, "Inverse scattering using a joint norm-based regularization," *IEEE Transactions on Antennas and Propagation*, Vol. 64, 1373–1384, 2016.
9. Richmond, J., "Scattering by a dielectric cylinder of arbitrary cross section shape," *IEEE Transactions on Antennas and Propagation*, Vol. 13, No. 3, 334–341, 1965.
10. Peterson, A. F., et al., *Computational Methods for Electromagnetics*, IEEE Press, New York, 1998.
11. Dauphin, Y. N., et al., "Identifying and attacking the saddle point problem in high-dimensional non-convex optimization," *Advances in Neural Information Processing Systems*, 2933–3941, 2014.
12. Chen, X., "Subspace-based optimization method for solving inverse-scattering problems," *IEEE Transactions on Geoscience and Remote Sensing*, Vol. 48, No. 1, 42–49, 2010.